

Viscosity enhancement in the flow of hydrolysed poly(acrylamide) saline solutions around spheres: implications for enhanced oil recovery

J. A. Odell · S. J. Haward

Received: 16 March 2007 / Accepted: 14 August 2007
© Springer-Verlag 2007

Abstract We have studied dilute aqueous solutions of hydrolysed poly(acrylamide), in various ionic environments, in flow around single spheres and around two spheres aligned on the axis of flow. The spheres are held on flexible cantilevers, while the polymer solutions, or solvent, are drawn past at controlled flow rates. We estimate the specific viscosities of the various solutions as a function of the strain rate over strain rates encompassing both the shear thinning and extension thickening regimes. For flow of solutions without added salts around a single sphere, we observe shear thinning followed by a significant increase in the non-Newtonian viscosity with increasing strain rate. The shear thinning reduces the maximal extensional viscosities of the solutions, which has important implications regarding the effectiveness of hydrolysed poly(acrylamide) in oil field applications. For flow of polymer solutions around two axially aligned spheres, we observe a significant reduction in the non-Newtonian forces experienced by the downstream sphere in comparison to the upstream sphere. We consider that this is salient to the understanding of non-Newtonian viscosification in porous media flow.

Keywords Sphere · Extensional flow · Stagnation point · Viscosity · Polymer solution · Polyelectrolyte

Introduction

Understanding the behaviour of particles settling in non-Newtonian fluids is of fundamental relevance to many processes including oil, paint, detergent and cosmetic formulation. In addition, enhanced oil recovery (EOR) techniques often utilise non-Newtonian fluids such as polymer solutions in the flooding of porous oil fields. As these are usually simulated by packed beds of spheres or ballotini, understanding such complex cyclic flows of polymer solutions should begin with understanding the flow around a single sphere.

Leal et al. (1988) selected the case of a sphere falling along the axis of a cylindrical tube of double the sphere radius as a benchmark problem in viscoelastic flow. However, with hindsight, this may not be the best choice of design for such a study due to the transient approach to steady state and the severely limited range of accessible flow regimes governed by the density range of available spheres.

Additionally, such “falling sphere” experiments that have encompassed high Deborah number flow regimes have revealed various unexplained non-Newtonian phenomena, including “negative wakes” and “memory effects”, which become manifest when successive spheres are allowed to fall along the same path. These types of effects tend to vary tremendously depending on the composition of the solution under study (see e.g. Riddle et al. 1977; Bisgaard 1983; Jones et al. 1994; Arigo et al. 1995; Arigo and McKinley 1998).

Flow around a sphere contains extensional and shear contributions. Many of the described non-Newtonian phenomena are likely to be associated with the extensional flow fields around the wake of the sphere.

J. A. Odell (✉) · S. J. Haward
H.H.Wills Physics Department, University of Bristol,
Tyndall Avenue,
Bristol BS8 1TL, UK
e-mail: jeff.odell@bristol.ac.uk

In a previous publication, we have described a new technique to study flow around spheres whereby spheres are held on fine flexible cantilevers while polymer solutions are pumped past at controlled flow rates (Haward and Odell 2004). This approach forces the flow into steady state, allows a greater range of flow regimes to be accessed than is possible in a falling ball experiment and also allows the drag force on the spheres to be calculated from the cantilever bend. Dilute solutions of monodisperse atactic poly(styrene) in dioctyl phthalate (a-PS in DOP) were studied in flow around a single isolated sphere and around two axially aligned spheres. It was possible to measure the flow field around the single sphere and to correlate a reduction in flow velocity in the trailing wake with an increase in the birefringence in the wake and an increase in the apparent specific viscosity of the polymer solution above a critical Deborah number. The increase in birefringence and apparent specific viscosity were attributed to a coil \leftrightarrow stretch transition of the type envisioned by de Gennes (1974) and Hinch (1977). Oriented, or stretched, macromolecules serve to dramatically increase the apparent viscosity of the polymer solution.

For flow around two axially aligned spheres, the flow modification in the wake of the leading sphere was found to affect the flow field around the trailing sphere. As a result, the trailing sphere experienced a smaller increase in apparent specific viscosity than the leading sphere, providing an explanation for the “memory effect”, when the terminal velocity of spheres following a common path through a viscoelastic solution depends upon the time interval between them; see Bisgaard (1983), Jones et al. (1994) and others.

In the present paper, we employ the novel techniques described in our previous article to study the flow of dilute aqueous solutions of high molecular weight hydrolysed poly(acrylamide) (HPAA) in flow around an isolated sphere and around two axially aligned spheres. Results of falling sphere experiments with commercial aqueous polymer solutions have been much more widely reported in the literature than with idealised model polymer solutions and may have greater practical significance to industrialised applications such as EOR. Our results will therefore provide a link between our novel methods and the traditional falling sphere experiment as well as provide valuable information about the behaviour of HPAA solutions in stagnation point extensional flows around obstacles. The HPAA solutions have been prepared in aqueous solutions of various salts, as well as in deionised water, to give insight into the behaviour of the solutions in brine, which is commonly used to prepare solutions for EOR.

In a previous paper, we have reported results on identical HPAA solutions flowing through regular crystallographic

arrays of spheres and random porous media (Odell and Haward 2006). Our overall aim was to approach the behaviour of real porous media, such as in EOR, through successive experiments linking the benchmark problem of idealised solutions around spheres and through crystallographic arrays (Haward and Odell 2003, 2004) through to commercial solutions through random arrays of ballotini.

Experimental

Apparatus

The flow cells used in the experiments, called “single sphere” and “double sphere”, are shown schematically in Fig. 1. The glass spheres had diameter 2 ± 0.02 mm and were supplied by Sigmund-Lindner of Germany. The cantilevers were in fact lengths of optic fibre of diameter 125 ± 2 μm . In the double sphere flow cell, the centre–centre sphere separation was 5 mm.

The cantilevers were cut to a length of ~ 35 mm, providing spring constants, k , of ~ 0.05 Nm^{-1} that would give a measurable displacement in flowing water. The spring constant was determined in situ by attaching the flow cell rigidly to a magnetic coil driven by a signal generator, exciting the first resonant frequency, ω , of the cantilever and using $\omega = \sqrt{k/m}$, where m is the mass of the sphere. Static load experiments at large deformations ensured that k would be constant over the experimental range of movement.

The flow was generated using a vacuum pump system, described by Haward and Odell (2004), to provide a non-pulsatile and easily controllable volume flow rate, U , and also to minimise mechanical degradation of the polymer solutions.

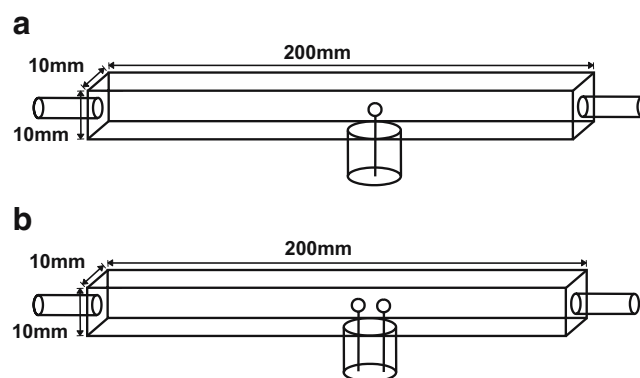


Fig. 1 **a** Schematic diagram of the single sphere flow cell; **b** schematic diagram of the double sphere flow cell. The spheres were 2 ± 0.02 mm in diameter, and the centre–centre spacing between spheres was ~ 5 mm

The Reynolds number of the flow was calculated using:

$$Re = \frac{\rho v r}{\eta} \quad (1)$$

Where ρ is the density of the solvent, v is the superficial flow velocity ($=U/\text{cross-sectional area of flow cell}$), and r is the radius of the spheres. For polymer solutions, the strain rate was determined by:

$$\dot{\epsilon} \approx \frac{v}{r} \quad (2)$$

A CCD video camera was used, enabling the displacement of the spheres to be measured directly as a function of Re or $\dot{\epsilon}$. The force experienced by the spheres was calculated using Hookes law. For polymer solutions, an estimate of the apparent specific viscosity, η_{sp} , was made by comparing the force exerted on the sphere by the polymer solution, F_{solution} , with that exerted by water, F_{water} at the same flow rate, i.e.:

$$\eta_{sp} = \frac{F_{\text{solution}} - F_{\text{water}}}{F_{\text{water}}} \quad (3)$$

F_{water} is generally well-fitted by a quadratic expression in Reynolds number, Re . The linear term corresponding to viscous contributions and the square term to inertial effects. The quadratic fit is subsequently taken as F_{water} . As the solution density is essentially equal to that of water, Eq. 3 effectively removes inertial contributions from F_{solution} and from the apparent specific viscosity, η_{sp} .

This method has the important advantage of eliminating the need to correct F_{solution} and F_{water} for inertial effects, as the inertial contributions will be essentially equal in both cases and will be removed by the process of subtraction in Eq. 3. Furthermore, in the case of the double sphere flow cell, Eq. 3 should eliminate any effects due to slipstreaming, as the slipstreaming will also be present in the case of water.

Solutions

Characterisation

The HPAA sample used in this study was ALCOFLOOD 1175A, supplied by Allied Colloids, Suffolk, VA. The molecular weight was very high (nominally $M_w=18 \times 10^6$, with $M_w/M_n \approx 2$) and the degree of hydrolysis between 0.35 and 0.4. Despite the importance of this type of polymer in industrial applications, including EOR, there is little literature relating to the characterisation of HPAA in solution, particularly with varying salt concentration and valence. The broad molecular weight distribution of the polymer also means that any characterisation that is possible will only apply to the peak of the distribution, with the high molecular weight tail remaining a largely unknown quantity.

Muller et al. (1979) have demonstrated that under specific solvent conditions (0.5 M NaCl), the HPAA molecule adopts similar behaviour and conformational properties to its non-ionic counterpart, poly(acrylamide) or PAA. Therefore, we can confidently make certain assumptions about HPAA solution properties based on the known molecular parameters of PAA.

Scholtan (1954) and Klein and Conrad (1980) provide values for the Mark–Houwink coefficients for PAA in H_2O which yield values for the intrinsic viscosity, $[\eta]$, for an $M_w=18 \times 10^6$ molecule of 4,020 $\text{mL} \cdot \text{g}^{-1}$ and 3,122 $\text{mL} \cdot \text{g}^{-1}$, respectively. Klein and Conrad also provide data for PAA in 0.5 M NaCl and in ethylene glycol at 25 °C (theta conditions), yielding $[\eta]=2,775$ and 11 $\text{mL} \cdot \text{g}^{-1}$, respectively. The values of intrinsic viscosity show that the PAA random coil is relatively highly expanded in either H_2O or in 0.5 M NaCl when compared with its conformation at theta conditions.

Molecular parameters available from Brandrup and Immergut (1989) for PAA in water at 30 °C allow calculation of the contour length (55.8 μm), radius of gyration (174 nm) and the equilibrium end–end length (427 nm). The ratio of contour length to end–end distance shows a strain to full extension of >100 , indicating that a coil \leftrightarrow stretch transition could be expected in a sufficiently strong velocity gradient.

From the radius of gyration, $R_g=174$ nm, we can estimate the overlap concentration for the $M_w=18 \times 10^6$ HPAA molecule in 0.5 M NaCl as $c^*=0.07\%$. This is based on each molecule occupying a cube of side $2R_g$. Our experimental concentration range spans $c^*/35 < c < c^*/9$. For our preferred concentration of $c=0.004\%$, $c/c^* \sim 1/20$. The overlap concentration will decrease with salt concentration as the polymer coil expands; however, our conservative estimates of c^* indicate that our test solutions should be considered highly dilute.

The value of $[\eta]$ from Klein and Conrad (1980) for PAA in 0.5 M NaCl can be used to calculate approximate values for the relative viscosities, η_{rel} , of HPAA in 0.5 M NaCl solutions at the experimental polymer concentrations (giving $1.05 < \eta_{rel} < 1.22$) For $c=0.004\%$, $\eta_{rel}=1.11$. These solutions therefore probably have shear viscosities very similar to water and are unlikely to show much shear thinning. In lower concentrations of salt, the HPAA molecule will become expanded by the increased effect of mutual repulsion along the chain. The effect of this should be to increase the shear viscosity of the solution and reduce the flexibility of the HPAA molecules; see, e.g. Durst et al. (1981).

Due to the high polydispersity index of the HPAA sample used, it is not possible to accurately define a value for the molecular relaxation time, τ . This means that a given strain rate will provide a wide range of values of Deborah number, De , and Weissenberg number, We . Previous experiments with well-defined polymer solutions have also

shown that the De for flow around spheres does not correspond well with theoretical predictions of the requirements for polymer stretching (Haward and Odell 2004). We believe that this is mainly due to the divergence of the flow field around the sphere. Considering these two issues in unison, we believe it is preferable not to consider De or We in this case; we quote only the strain rate, based on the flow geometry and defined by Eq. 2.

Preparation

Solutions were prepared at polymer concentrations of $0.008\% \geq c \geq 0.002\%$. The monovalent salt used was NaCl in concentrations between 1 mM and 0.5 M. Several analytical grade divalent and multivalent salts were used: $MgSO_4$, $MgCl_2$, $CaCl_2$, $BaCl_2$, and $SrCl_2$, $ZnCl_2$, $AlCl_3$ and $FeSO_4$, all supplied by Riedel-de Haen, Seelze, Germany.

The solutions were prepared in beakers containing 3 l of distilled deionised water of pH 6 ± 0.5 . When the salt had completely dissolved, a vortex was created in the brine using a magnetic stirrer, and the required amount of HPAAs powder was added. After a few seconds, when the polymer powder had dispersed in the brine, the stirring was reduced to the minimum speed to minimise mechanical degradation of the polymer during the following 24 h while the polymer completely dissolved. Before experimentation, the solutions were left to stand without stirring for half an hour. The temperature of the solutions, measured immediately before experimentation, was 22 ± 1 °C. None of the solutions showed any sign of gel formation or variation in refractive index, and no precipitation of polymer or salt was ever observed.

Results

Single sphere flow cell

Figure 2a shows the results of force measurements on the single sphere flow cell with 0.004% solutions of $M_w = 18 \times 10^6$ HPAAs in various aqueous solutions of NaCl where the solid line represents the data obtained from distilled deionised water.

Figure 2b shows the specific viscosity as a function of strain rate derived from the same data as Fig. 2a. For clarity, it should be pointed out that the definitions of Re and strain rate (given in Eqs. 1 and 2, respectively), the flow geometry and the density and viscosity of water coincidentally result that for a given superficial flow velocity, $Re = \dot{\epsilon}$. Throughout this paper and in all of the figures, the Reynolds number and the strain rate are numerically identical and effectively interchangeable.

It is seen in Fig. 2b that with no NaCl present, the solution has an initial high shear viscosity attributable to the

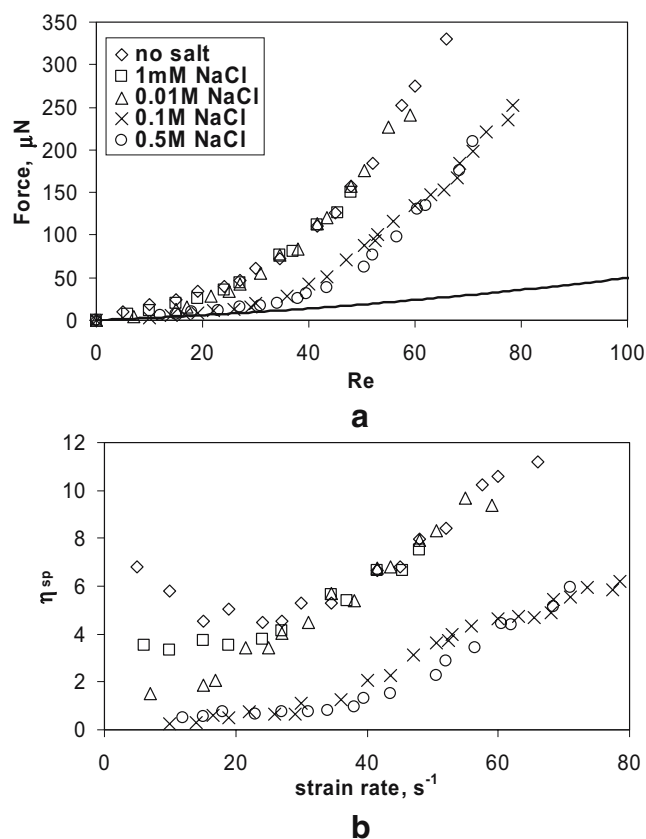


Fig. 2 **a** Drag force as a function of Reynolds number in the single sphere flow cell for a 0.004% solution of $M_w = 18 \times 10^6$ HPAAs in various aqueous solutions of NaCl. The solid line represents a quadratic fit to the data for pure water. **b** Specific viscosity as a function of strain rate derived from the data of Fig. 1a

extended nature of the unscreened high molecular weight HPAAs. The solution displays a degree of shear thinning before a non-Newtonian increase in the viscosity is observed with increasing strain rate $\dot{\epsilon}$. This shear thinning is in contrast to the results of Haward and Odell (2004) using model Boger fluid solutions of atactic poly(styrene) (a-PS). At higher strain rates, the solution shows thickening behaviour similar to that reported on a-PS and associated with coil \leftrightarrow stretch transition behaviour in extensional components of the flow around the stagnation point in the wake.

As the concentration of NaCl in the solution is increased, the shear viscosity becomes reduced, the shear thinning behaviour is lost, and the increase in viscosity tends to occur at higher strain rates, indicating that the molecular relaxation time, τ , of the HPAAs decreases. With NaCl present, the HPAAs solutions show behaviour qualitatively similar to that observed with solutions of randomly coiled polymer molecules (Haward and Odell 2004). The viscosity and relaxation time reducing effects of the salt appear to have become saturated at 0.1 M concentration, at which point, a reduction in the maximum achievable value of specific viscosity also occurs.

The behaviour of the HPAA solutions in the presence of NaCl is, in general, in line with expectations (e.g. Durst et al. 1981) and can be explained by the effects of Na⁺ counter ions in the solution screening the negative charges on the polymer chain, resulting in a contraction of the coils and an increase in the relaxation time. However, the reduction in the plateau value of η_{sp} for NaCl concentrations between 0.01 and 0.1 M is an unexpected observation. It is odd that plateau values are affected by monovalent salt.

The effect of polymer concentration on the viscosities of HPAA solutions in the presence of 0.5 M aqueous NaCl is shown by Fig. 3. Within experimental error, Fig. 3 shows an increase in plateau value of η_{sp} proportional to concentration, that is, broadly indicative of dilute solution behaviour, consistent with our estimates of c^* based on the molecular parameters of PAA in water.

Figure 4 shows the effect of increasing the concentration of the divalent salt CaCl₂ in a 0.004% solution of HPAA. The effect of the CaCl₂ on the properties of the solution is seen to be similar to, although more pronounced than, the effect of NaCl. In fact, 0.1 mM of CaCl₂ appears to have a greater viscosity reducing effect on the solution than 10 mM of NaCl, which is surprising. As the concentration of CaCl₂ is increased, the shear viscosity of the solution is reduced, the maximum extensional viscosity is reduced, and the increase in η_{sp} tends to occur at higher strain rate.

Further examples of the effects of divalent salts on HPAA solutions are shown in Fig. 5a and b. As the concentration of salt is increased, the effect of each salt is seen to be qualitatively similar to the effect of CaCl₂ described above. However, there are quantitative differences between the effect of each salt; for example, MgSO₄ consistently has a smaller effect than the other salts and SrCl₂, and BaCl₂ generally have the strongest effect.

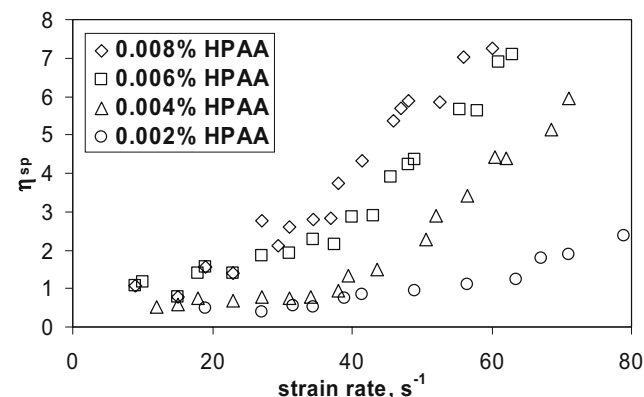


Fig. 3 Specific viscosity as a function of strain rate in the single sphere flow cell for solutions of various concentration of $M_w=18 \times 10^6$ HPAA in 0.5 M aqueous solutions of NaCl

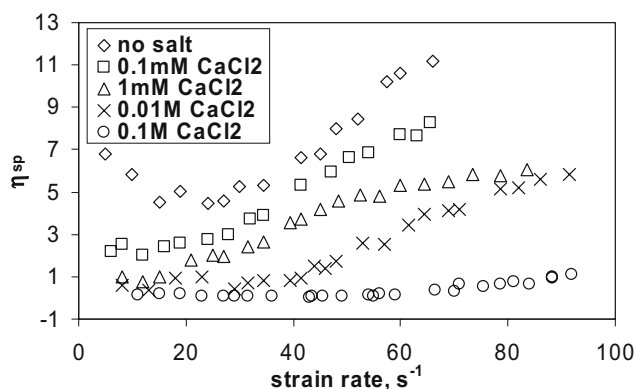


Fig. 4 Specific viscosity as a function of strain rate in the single sphere flow cell for a 0.004% solution of $M_w=18 \times 10^6$ HPAA in various aqueous solutions of CaCl₂

degree of hydration of the positive counter ion or by the valency of the anion, which may explain the different properties of solutions containing MgCl₂ compared with MgSO₄.

Figure 6 shows how the specific viscosity varied with strain rate for a 0.004% solution of HPAA prepared in “synthetic brine”. The “synthetic brine” was produced from distilled deionised water containing the following quantities

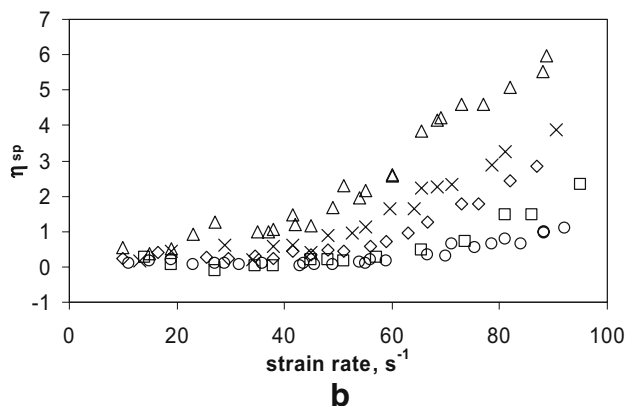
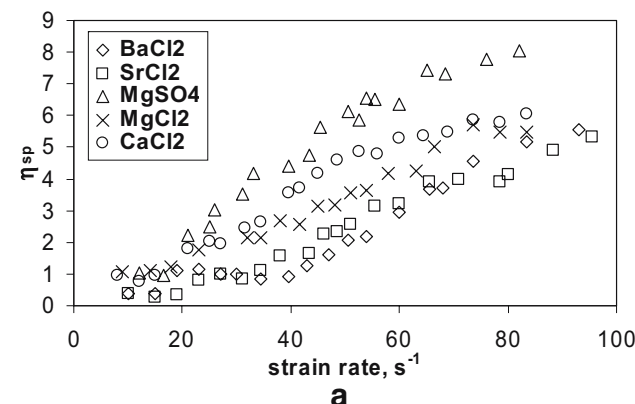


Fig. 5 Specific viscosity as a function of strain rate in the single sphere flow cell for a 0.004% aqueous solution of $M_w=18 \times 10^6$ HPAA in the presence of various divalent salts at concentration: **a** 0.001 M, **b** 0.1 M

of salts: 0.46 M NaCl, 0.052 M MgCl₂, 0.01 M CaCl₂, 0.00015 M SrCl₂, 5×10^{-5} M AlCl₃, 3.6×10^{-7} M BaCl₂, 1.8×10^{-7} M FeSO₄, 1.5×10^{-7} M ZnCl₂. These are the molar concentrations of the eight most abundant salts present in the sea, according to Hodgman (1960–1961). Previous results for 0.004% HPAA in 0.5 M NaCl and 0.1 M CaCl₂ are also shown in Fig. 6 for ease of comparison.

The curve obtained with the synthetic brine solution lies slightly above the curve obtained with a 0.1 M CaCl₂ solution, but well below that obtained with a 0.5 M NaCl solution, which might be expected to show similar behaviour to an aqueous solution of neutral poly(acrylamide). This result has a definite relevance to enhanced oil recovery in applications where HPAA polymers are prepared using seawater as a solvent. Our results suggest that a poly(acrylamide) with a low degree of hydrolysis may be a more effective viscosifier for brine than hydrolysed poly(acrylamide), as it should not be so greatly affected by divalent and multivalent cations (see “General discussion” below).

Double sphere flow cell

Figure 7a shows how the force exerted on each ball in the double sphere flow cell increases with the Reynolds number in pure water and a 0.004% solution of $M_w = 18 \times 10^6$ HPAA in deionised water. Both curves for water in Fig. 7 are again well fitted by quadratics in Re. The curve representing the force on sphere 2 lies slightly below that of sphere 1, which is presumably due to slipstreaming effects. However, the difference between the forces felt by spheres 1 and 2 in the HPAA solution is clearly far greater than the effect of slip streaming observed in water.

When the curves in Fig. 7a are transformed into plots of the specific viscosity, the nature of the different responses of each sphere to the flowing HPAA solution become much clearer (Fig. 7b). Within experimental error, the specific

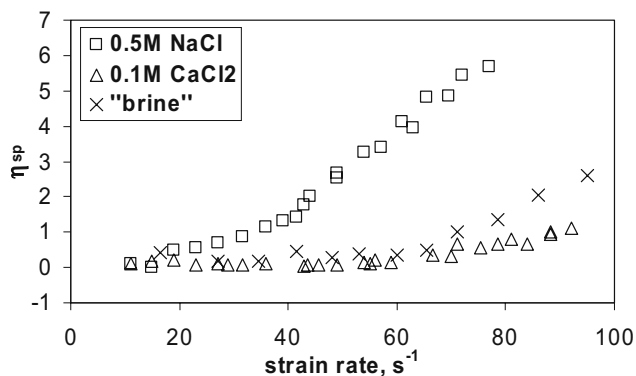


Fig. 6 Specific viscosity as a function of strain rate in the single sphere flow cell for a 0.004% solution of $M_w = 18 \times 10^6$ HPAA in various aqueous solutions

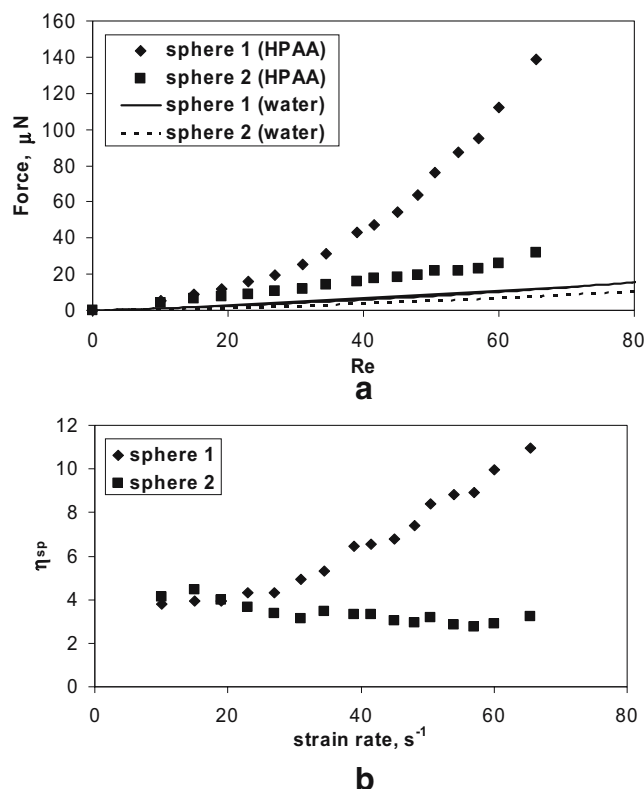


Fig. 7 **a** Drag force on each sphere of the double sphere flow cell as a function of Reynolds number for a 0.004% solution of $M_w = 18 \times 10^6$ HPAA in deionised water. The *lines* represent quadratic fits to the data for pure water. **b** Specific viscosity as a function of strain rate derived from the data of **a**

viscosity vs strain rate curve for sphere 1 is very similar to that obtained from the same solution in the single sphere flow cell shown in Fig. 2b, i.e. a gradual increase in η_{sp} with increasing strain rate, although here, we do not observe the shear thinning. However, sphere 2 displays very different behaviour, effectively showing a constant value of η_{sp} over the whole strain rate range. At low strain rate, there is no change to or orientation of the fluid as it passes sphere 1 so that sphere 2 experiences fluid of the same specific viscosity. However, for $\dot{\epsilon} > 30 \text{ s}^{-1}$, the two curves begin to diverge, and sphere 2 experiences a dramatically reduced specific viscosity compared with sphere 1. This effect is equivalent to the “memory effect” briefly described in the “Introduction” whereby in falling ball experiments with viscoelastic liquids, the terminal velocities of falling spheres are seen to increase as subsequent spheres are dropped (e.g. Bisgaard 1983; Jones et al. 1994). The behaviour is also similar to, although more extreme than that observed by Haward and Odell (2004) in dilute solutions of monodisperse a-PS in DOP.

Figure 8 shows the specific viscosity as a function of strain rate for a 0.004% solution of HPAA in 0.5 M aqueous NaCl. Sphere 1 shows behaviour very similar to that observed with the same solution in the single sphere

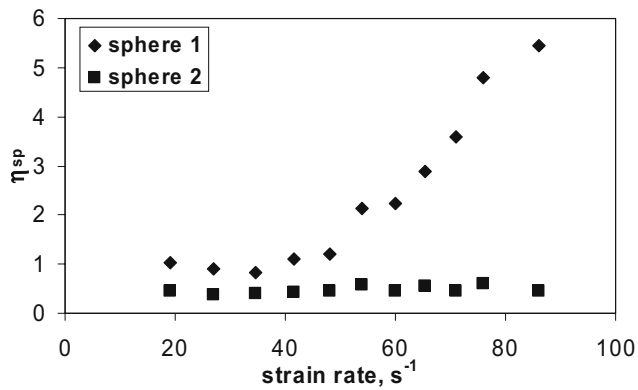


Fig. 8 Specific viscosity as a function of strain rate in the double sphere flow cell for a 0.004% aqueous solution of $M_w=18 \times 10^6$ HPAA in the presence of 0.5 M NaCl

flow cell, see Fig. 2b. As in Fig. 7b, sphere 2 shows a constant value of η_{sp} with strain rate.

Figure 9 shows how the specific viscosity varies with strain rate in a 0.004% solution of HPAA in 0.1 M aqueous CaCl_2 .

Figure 10 shows the difference in specific viscosity between the leading and trailing spheres for 0.004% solutions of HPAA in deionised water, 0.5 M NaCl, and 0.1 M CaCl_2 .

General discussion

There are differences between the falling ball experiment, which is transient, and the present study, which forces the flow into a steady state (and is therefore more comparable to the situation in EOR). In the double sphere experiment we conduct here, a constant given flow rate results in a fixed separation between the spheres, although the force on each sphere may be very different. In the falling ball experiment, the difference in viscous force on each sphere results in the spheres having different velocities, so the separation between the spheres will change as a function of time as the spheres fall. Normally, the separation between

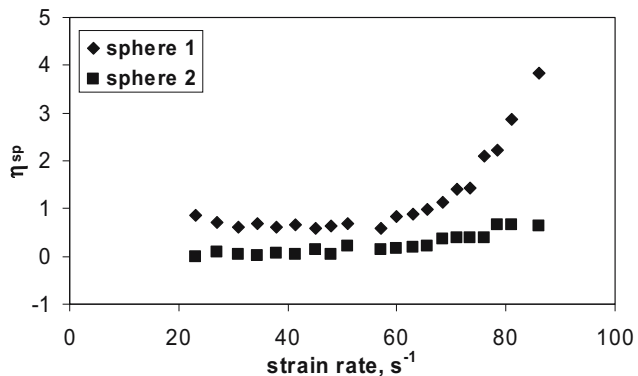


Fig. 9 Specific viscosity as a function of strain rate in the double sphere flow cell for a 0.004% aqueous solution of $M_w=18 \times 10^6$ HPAA in the presence of 0.1 M CaCl_2

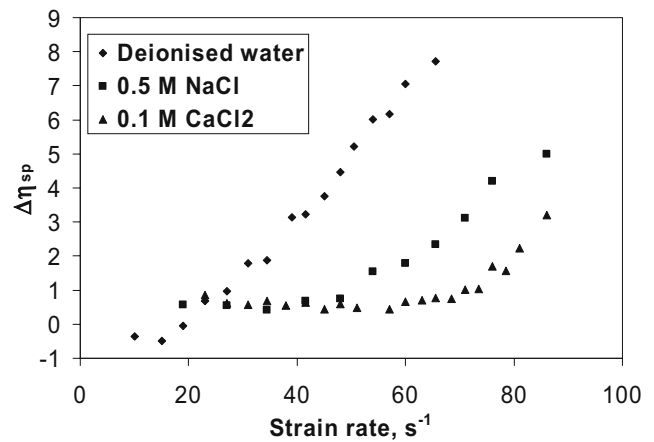


Fig. 10 Difference in specific viscosity between spheres 1 and 2 for flow of 0.004% HPAA in the aqueous salt solutions indicated

the falling spheres decreases, as the trailing spheres usually fall faster than the first. It has been found that this effect diminishes with increasing separation between spheres (e.g. Bisgaard 1983). Therefore, as two falling spheres approach each other in a polymer solution, it can be assumed that the second sphere will continue to accelerate. Provided the initial separation between the spheres is sufficiently close to produce an effect on the second sphere, the second sphere may never achieve steady state, or terminal velocity, and may continue to accelerate until eventually converging with the sphere in front. This was observed by Riddle et al. (1977).

A drawback of our experiment is that we have no independent control of the separation between the spheres in the double sphere experiment. Increasing the flow rate results not only in a higher strain rate but also in a reduced time for flow between the spheres in the falling ball analogy; therefore, the effect is similar to increasing the density of spheres and reducing the time interval between them. Our experiment could be adapted to allow a variable separation between spheres for a fixed flow rate, allowing a more detailed study of the interaction between the spheres.

As the HPAA molecule has a very low intrinsic birefringence, direct evidence of polymer stretching in the wake of the sphere is difficult to achieve in dilute solutions. However, the specific viscosity curves for the HPAA solutions with added salts, in “Single sphere flow cell”, are of the same qualitative form as those observed for a-PS solutions (Howard and Odell 2004), so it is reasonable to assume that the increase in viscosity with increasing strain rate in HPAA solutions is also due to the coil↔stretch transition. The use of birefringent aqueous systems such as poly(ethylene oxide) or poly(styrene sulphonate) could confirm this. We can be sure that the effects we report here are not inertial due to our treatment of the data in Eq. 3. Effectively, therefore, the effects we observe must be viscoelastic in origin.

The principal effects of salts on the HPAA solutions are to reduce the shear viscosity and relaxation time of the solution, resulting in a more critical coil \leftrightarrow stretch transition. The effect of divalent salts on the solution is more significant (by at least an order of magnitude) than the effect of monovalent NaCl for a given molar salt concentration. At high salt concentrations, the maximum achievable extensional viscosity of the solution may also be reduced compared to the value obtained for HPAA in deionised water.

The effect of the divalent salts upon the polyelectrolyte properties is thought to be substantially greater than the effect of monovalent NaCl due to the formation of intra-molecular bridges, which would have the effect of contracting the polymer coil and causing a decrease in the relaxation time (Miles et al. 1983). If the intra-molecular ionic bridges are strong enough to maintain the molecular stress in the extensional flow field, the HPAA molecules could become effectively “locked” into a coiled configuration and be unable to extend significantly.

If different divalent cations form intra-molecular bridges of different “strengths”, then this explanation could account for the differences between the properties of HPAA solutions with different added divalent salts. Indeed, the strength of the ionic bridge will depend upon the solubility of the succinate-type salt, which is likely to be formed between a divalent cation and an HPAA molecule. If the succinate salt is highly insoluble, such that the time scale for the existence of intra-molecular bridges is high compared to the polymer relaxation time, the extensibility of the polymer chain could be seriously reduced. The more soluble the bond between the HPAA molecule and the cation, the more transient the intra-molecular bridge would be, and the effect of the bond on HPAA coil would be correspondingly less.

The solubility of succinate salts is found to decrease with the increasing molecular weight of the cation, see Washburn (1926–1933), and therefore provides a possible explanation for our results. It should be noted that Miles et al. (1983) have offered a similar explanation based on the formation of ionic salts for the behaviour of poly(styrene sulphonate) solutions in the presence of various divalent salts.

The powerful effect of the synthetic “brine” at reducing the viscosifying properties of HPAA (similar to 0.1 M CaCl₂, see Fig. 6) is likely to be due to the ability of divalent and multivalent ions to cross-link the coil, reducing its inherent extensibility. Higher flow rates may then be required to stretch macromolecules and provide significant viscosity enhancement. This might be a disadvantage to the use of highly hydrolysed PAA for oil field flooding, especially when taken together with previous data on the severe thermo-mechanical degradation of HPAA in the

presence of salts and at modest temperatures (Muller 1981; Noik et al. 1995; Odell and Haward 2006).

The results of the experiments on flow around two spheres (Figs 7, 8, 9 and 10) are of particular relevance to the understanding of porous media flows, or at least to model porous media that consist of beds of spheres or ballotini. In the random geometry of a bed of spheres, many particles are likely to occupy locations more or less directly downstream from the stagnation points of preceding particles, just as the second of the two spheres in our experiment is situated downstream from the stagnation point of the first. At least in an idealised sense, our flow geometry can be thought of as mimicking this particular aspect of flow through such model porous media. The results from our experiments, both here and previously (Haward and Odell 2004), show that where this kind of geometry arises, downstream particles will experience a relatively smaller increase in apparent extensional viscosity when the critical strain rate is exceeded.

These considerations may have consequences regarding the way porous media are modelled experimentally, i.e. by randomly packed beds of spheres. In such geometries, the trailing stagnation points of many spheres are likely to occupy ineffective locations within the flow field, and as a result, may not contribute greatly to the non-Newtonian viscosification process. Real porous media in sedimentary layers may well present more effective stagnation points at bifurcations and pore entrances and, in this respect, may not be well modelled by closely packed beds of spheres or ballotini.

However, our results using HPAA solutions in crystallographic porous media with and without stagnation points have indicated that stagnation points in the array *do* contribute significantly to the viscosification (Odell and Haward 2006). This was attributed to the free-draining nature of the HPAA coil and its consequent inability to become highly stretched in a cyclical flow from pore to pore. However, it is possible that stagnation points are only required for the initial stretch and that pore-space variations are then able to maintain the extended conformation. This is similar to the speculation that pre-stretched conformations are important in producing an overall viscosification effect in cyclical flows of idealised polymer solutions through crystallographic arrays reported previously (Haward and Odell 2003).

Conclusions

We have observed non-Newtonian increases in specific viscosity with increasing strain rate for HPAA solutions in different salt environments. This is similar to that observed in idealised solutions of a-PS/DOP observed by Haward and Odell (2004), which correlated with an increase in the birefringence in the trailing wake of the sphere. This

implies that the cause of the viscosification in HPAA solutions is also polymer orientation/extension in the trailing wake, i.e. a coil↔stretch transition in the stagnation point of the sphere. This mechanism of viscosity increase will pertain in porous media and sedimentary layers wherever there are extensional components (at bifurcations and pore entrances) and stagnation points (at surfaces and where flows converge). It is likely to be key to the effectiveness of such solutions in polymer flooding in EOR.

The addition of increasing amounts of the monovalent salt NaCl to the solution has the expected effect of gradually reducing the shear viscosity of the solution. This results in greater criticality of the dilatant behaviour, which lends weight to the coil↔stretch transition, being the origin of this effect. At high molar concentrations, the addition of NaCl also appears to reduce the maximum extensional viscosity of solution, which is unexpected.

The addition of increasing amounts of divalent salts to the solution results in a very rapid reduction in both the shear and extensional viscosities of the solutions, probably due to the formation of intra-molecular bridges.

The effect of mixtures of monovalent, divalent and multivalent salts (or synthetic brine) on the non-Newtonian viscosity of HPAA solutions is particularly severe, dramatically reducing the shear and extensional viscosities achievable. This raises doubts about the effectiveness for EOR of highly hydrolysed HPAA in a brine environment. Non-ionic PAA may be more effective in the presence of multivalent salts at concentrations that occur in brine.

The interactions observed between the two spheres of the double sphere flow cell indicate that where similar geometries arise in model porous media, there may be a significant reduction in the contribution of downstream spheres to the extensional flow field, i.e. in producing a non-Newtonian increase in the fluid viscosity. As such, packed beds of spheres may not be the best way of modelling real oil-bearing sedimentary layers.

Acknowledgements We gratefully acknowledge the support of the EPSRC and the EU Alfa programme and helpful discussions with Prof A.J. Muller.

References

Arigo MT, McKinley GH (1998) An experimental investigation of negative wakes behind spheres settling in a shear-thinning viscoelastic fluid. *Rheol Acta* 37:307–327

- Arigo MT, Rajagopalan D, Shapley N, McKinley GH (1995) The sedimentation of a sphere through an elastic fluid. Part I. Steady motion *J Non Newtonian Fluid Mech* 60:225–257
- Bisgaard C (1983) Velocity fields around spheres and bubbles investigated by laser-Doppler velocimetry. *J Non Newtonian Fluid Mech* 12:283–302
- Brandrup J, Immergut EH (eds) (1989) *Polymer handbook*, 3rd edn. Wiley Interscience, USA
- de Gennes PG (1974) Coil-stretch transition of dilute flexible polymers under ultrahigh velocity gradients. *J Chem Phys* 60:5030–5042
- Durst F, Haas R, Kaczmar BU (1981) Flows of Dilute hydrolyzed polyacrylamide solutions in porous media under various solvent conditions. *J Appl Polym Sci* 26:3125–3149
- Haward SJ, Odell JA (2003) Viscosity enhancement in non-Newtonian flow of dilute polymer solutions through crystallographic porous media. *Rheol Acta* 42:516–526
- Haward SJ, Odell JA (2004) Molecular orientation in non-Newtonian flow of dilute polymer solutions around spheres. *Rheol Acta* 43:350–363
- Hinch EJ (1977) Mechanical models of dilute polymer solutions in strong flows. *Phys Fluids* 20:S22–S30
- Hodgman CD (ed) (1960–1961) *Handbook of Chemistry and Physics*, 42nd edn. The Chemical Rubber Publishing Company, Cleveland, USA
- Jones WM, Price AH, Walters K (1994) The motion of a sphere falling under gravity in a constant-viscosity elastic liquid. *J Non-Newtonian Fluid Mech* 53:175–196
- Klein J, Conrad K (1980) Characterisation of poly(acrylamide) in solution. *Macromol Chem* 181:227–240
- Leal LG, Denn MM, Keunings R (1988) Lake Arrowhead workshop special issue papers—introduction. *J Non-Newtonian Fluid Mech* 29:1–8
- Miles MJ, Tanaka K, Keller A (1983) The behaviour of polyelectrolyte solutions in elongational flow; the determination of conformational relaxation times (with an Appendix of an anomalous adsorption effect). *Polymer* 24:1081–1088
- Muller G (1981) Thermal stability of high-molecular-weight polyacrylamide aqueous solutions. *Polym Bull* 5:31–37
- Muller G, Laine JP, Fenyo JC (1979) High-molecular-weight hydrolyzed polyacrylamides. I. Characterization. Effect of salts on the conformational properties. *J Polym Sci Polym Chem Ed* 17:659–672
- Noik CH, Delaplace PH, Muller G (1995) Physio-chemical characteristics of polyacrylamide solutions after mechanical degradation through a porous medium. *Proceedings of the International Symposium on Oilfield Chemistry*, pp 93–100
- Odell JA, Haward SJ (2006) Viscosity enhancement in non-Newtonian flow of dilute aqueous polymer solutions through crystallographic and random porous media. *Rheol Acta* 45: 853–863
- Riddle MJ, Narvaez C, Bird RB (1977) Interactions between two spheres falling along their line of centres in a viscoelastic fluid. *J Non-Newtonian Fluid Mech* 2:23–35
- Scholtan W (1954) The determination of the molecular weight of polyacrylamide by means of the ultracentrifuge. *Makromol Chem* 14:169–178
- Washburn EW (ed) (1926–1933) *International critical tables*. McGraw-Hill Book Company Inc., New York, USA